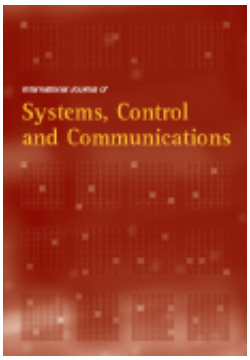

International Journal of Systems, Control and Communications

ISSN online: 1755-9359 - ISSN print: 1755-9340
https://www.inderscience.com/ijscc

Design and experimental evaluation of global sliding mode controller

A.R. Laware, A.K. Patil, V.S. Bandal, D.B. Talange

DOI: 10.1504/IJSCC.2022.10048704

Article History:
Received: 17 April 2021
Accepted: 17 December 2021
Published online: 06 December 2022

Design and experimental evaluation of global sliding mode controller

A.R. Laware*

Department of Electrical Engineering,
Dr. Vithalrao Vikhe Patil College of Engineering,
Ahmednagar – 414111, India
Email: ajitlaware2003@gmail.com
*Corresponding author

A.K. Patil

Department of Electronics and Telecommunication Engineering,
Dr. Vithalrao Vikhe Patil College of Engineering,
Ahmednagar – 414111, India
Email: anitamdhoke@gmail.com

V.S. Bandal

Government Polytechnic,
Pune, India
Email: vitthalsbandal@gmail.com

D.B. Talange

Department of Electrical Engineering,
College of Engineering,
Pune, India
Email: talanged@gmail.com

Abstract: The paper considered real-life applicability of global sliding mode controller (GSMCr) for nonlinear uncertain tank process. In a typical sliding mode control (SMC), robustness during reaching phase is not guaranteed. The proposed strategy interrogates the reaching phase, mitigates chattering, and overcomes external disturbances. The control law input has been formulated based on minimum and maximum values of estimated system parameters to alleviate chattering effect. Direct Lyapunov function confirms the stability condition. Proposed method has been designed and implemented to realise a smooth sliding manifold. The efficacy is demonstrated experimentally for laboratory single input single output level control system as well as second-order uncertain servo plant via the simulation tests. The reported results affirm the superiority of control method over typical SMC in terms of speed of process and time-domain specifications. The real-time implementation guarantees the robustness in terms of multi-level set-point changes, parameter variations and disturbance rejection. It shows 33.33% improvements in process variable deviations and 10.71% reduction in chattering as compared to conventional SMC. The simulation example shows 8.51% chattering reduction over prevalent SMC.

Keywords: global sliding mode controller; GSMCr; modelling; identification; control; real-time experimentation.

Reference to this paper should be made as follows: Laware, A.R., Patil, A.K., Bandal, V.S. and Talange, D.B. (2023) 'Design and experimental evaluation of global sliding mode controller', *Int. J. Systems, Control and Communications*, Vol. 14, No. 1, pp.40–59.

Biographical notes: A.R. Laware received his BE in Instrumentation and Control Engineering from Government College of Engineering, Jalgaon, India in 2000 and ME in Instrumentation and Control Engineering from Pune University in 2007. He completed his PhD in Electrical Engineering from Pune University, Pune, India in 2020. His research interests include control system design, sliding mode controller synthesis and its optimisation.

A.K. Patil received her BE in Electronics and Telecommunication Engineering from GCOE, Dhule, India in 1996 and ME in Electronics and Telecommunication Engineering from JNEC, Aurangabad in 2006. She has done his PhD in Electronics and Telecommunication Engineering from North Maharashtra University, Jalgaon, India in 2016. Her research interests include wireless communication systems and internet of things.

V.S. Bandal received his BE and ME in Electrical Engineering from Government College of Engineering, Karad, India in 1989 and 1995 respectively. He received his PhD from System and Control Engineering department, IIT Bombay, India in 2006. Currently, he is a Principal at the Government Polytechnic, Pune, India. He has published about 100 referred journal and conference papers. His research interest covers modelling of dynamical systems, robust control of large scale systems, power system stabiliser and sliding mode control. He received research grants from AICTE, DST, BARC and BRNS. He is a member of IEEE, ISTE and IET.

D.B. Talange received his BE and ME in Electrical Engineering from the Walchand Engineering College, Sangali, India and Victoria Jubilee Technical Institute, Matunga, Bombay-19, India, in 1981 and 1983 respectively. He received his PhD from System and Control Engineering department, IIT Bombay, India in 2005. Currently, he is a Professor and the Head of Electrical Engineering Department at the College of Engineering, Pune, India. He has published about 100 referred journal and conference papers and 12 books. He has filed and published four patents. His research interest covers nuclear engineering, robust control, and process plant control. He received research grants from AICTE, DST, BARC and BRNS. He is a member of IEEE, ISTE and IET.

1 Introduction

Sliding mode control (SMC) is an impressive control strategy for controlling uncertain systems such as tank levels, automotive, reactors, etc. It is originated from variable structure control (VSC) in early 1950s and elaborated by Emelyanov (1967) and Itkis (1976). The major features of SMC are: invariance and robustness concerning system parameter variations, and unknown disturbances. Hung et al. (1993) discussed the theory of SMC, main results and practical applications. Despite invariance and robustness,

typical SMC has some drawbacks such as large control input magnitude and chattering in control signal. Controller robustness depends on the saturation limit of control signal. The saturation should not be ignored through practical point of view.

Errami et al. (2016) explored variable structure-based SMC for the variations of wind speed. The performance of variable speed wind energy system under different conditions and grid fault was investigated using simulation tests which devised the superiority of proposed strategy.

To solve this problem, with the bounded control input, Slotine and Spong (1985) estimated region of asymptotic stability. However, chattering was unsolved issue of proposed strategy. Hence, Lu and Chen (1995) analysed global sliding mode controller (GSMCr) which guarantees the sliding condition over complete output. To enact fast tracking, Choi and Park (1997), Ashchepkov (1983) and Chern and Wu (1992) have proposed moving sliding surfaces, optimal sliding surface and optimal linear regulator techniques respectively. However, during reaching mode, the controller performance to uncertainties and external disturbances may not be satisfied.

Liu (2006) proposed a backstepping SMC and global SMC for three-axis flight servo system to reduce the error between nominal model and practical plant in which robustness is guaranteed by GSMCr while steady-state accuracy is obtained with integral backsteeping control law. A global SMC for an intra-aortic balloon pump was designed by Chang and Gao (2010). To reduce the chattering, disturbance compensator is used. The accuracy of flow probe affects system performance. Uswarman et al. (2014) focused the stabilisation problem of magnetic levitation system using global SMC and conventional SMC. They reported that range of parametric uncertainties is limited and chattering is the main issue.

To guarantee the global convergence and reaching phase elimination, a dummy variable is added to original sliding surface by Lu and Chen (2007) for robot manipulator system. Still, the magnitude of control efforts is large and chattering issues are unsolved. Choi et al. (2001) presented global SMC for brush less motor using bounded control input which yields smooth operation. It is more robust as compared to classical SMC as revealed by experimental tests.

The global SMC-based two link manipulator system was explored by Lu and Chiu (2009). It is investigated to assign closed-loop real eigenvalues. Though the eigenvalues are real, it gives sluggish responses. The work involves a formulation of GSMCr strategy in presence of parametric uncertainties. Experimental tests were conducted to illustrate the control performance of proposed control design method.

Cai et al. (2013) designed global SMC with nonlinear integral sliding surface for a helicopter system. It eliminates the reaching phase of conventional SMC, overcomes the effect of unknown disturbance and input time-delay. The efficiency was devised by simulation tests. Mobayen (2015) designed GSMCr for under actuated systems to improve the robustness and stability of closed-loop system. Linear matrix inequalities (LMI) are used to derive the asymptotic stability conditions. Control input compels states of system exponentially to the sliding manifold. Simulations and illustrative example investigates the efficacy of proposed strategy.

Xiu et al. (2017) explored global fast SMC for quad-rotor unmanned helicopter. The exponential reaching law-based control input was derived. Direct Lyapunov function ensures the stability of the system. The simulation results reveal that global fast SMC has better response rate than conventional GSMCr design.

The researchers in Gandhi et al. (2013) and Gandhi and Bhole (2013) have explored process and its associated controls for latest technological trends in bulk lithography, micro stereo lithography, and 3D printing which devise the control of gun ink, speed of ink injection and temperature control of resign layers. Gandhi et al. (2013) presented microstereolithography technique to optomechatronic requirements which includes the design goals such as high resolution and high speed fabrication. They demonstrated system integration and process parameters for the fabrication of large micro components.

Gandhi and Bhole (2013) devised experimental characterisation for two resin systems of unconstrained depth photo polymerisation process to Gaussian layer beam. They proposed empirical model which represent non-dimensional depth variation with respect to time and energy of resins. The advantages of bulk lithography have been highlighted.

The design and implementation of wireless-based DC motor controlling and monitoring system were proposed by Anumula et al. (2017). They illustrated the direction and speed control with MSP430 controller and H-bridge converter with overload factor of DC motor. Singh and Padhy (2017) presented a second order SMC fused with PI-PD structure for inverted pendulum system to alleviate the chattering effect. Proportional-integral (PI) type sliding surface has been proposed to improve the performance. The simulation and experimental tests have been carried out to validate the controller.

A novel dynamic SMC based on fractional calculus has been proposed for control and synchronisation of Lorenz-Stenflo (LS), and Qi fractional chaotic systems with matched disturbances in Gholipour et al. (2021). They presented the said technique for the system order as low as 3.76 and 3.48. From the simulation tests, they explored the reduced chattering effect.

In this research article, global SMC design for controlling water level of tank system has been proposed. The minimum-time trajectory can be achieved with the bounded system parameters, controller output limits and reference input. The validation of performance has been verified via experimental tests. The proposed strategy has been compared with classical SMC method.

The considerable contribution of the work is to design GSMCr and testing in real-life. The classic features of SMC; insensitivity to parameter uncertainties, external disturbances and real-time implementation with global SMC make sliding surface smoother. It also alleviates the chattering effect.

The work is framed as: Section 2 presents the problem formulation and objective. Section 3 is devoted to design procedure of classical SMC and global SMC including stability analysis. The laboratory process description and modelling is covered in Section 4. Section 5 deals with real-time experimental results and discussions while Section 6 devises the robustness and disturbance analysis. The simulation work for second-order uncertain servo system with sinusoidal control input is illustrated in Section 7. Lastly, research work summary has been presented.

2 Problem formulation and objective

Consider the representation of nonlinear process as (Geng et al., 2013)

$$\begin{aligned} \dot{x}_1 &= x_2 \\ \dot{x}_2 &= a(a) + b(x)u(t) + w(t) \\ y &= x_1 \end{aligned} \tag{1}$$

where $x = [x_1, x_2]^T \in \Re$ is the state vector, $a(x)$ and $b(x)$ are the vector fields, $u(t)$ is the control input and $w(t)$ denotes the unknown disturbances.

The system dynamics can be written as

$$a(x) = a_0(x) + \Delta a(x) \tag{2}$$

$$b(x) = b_0(x) + \Delta b(x) \tag{3}$$

where $a_0(x)$ and $b_0(x)$ are the nominal (estimated) system dynamics. $\Delta a(x)$ and $\Delta b(x)$ are the modelling uncertainties. The bounded uncertainties must satisfy the following conditions (Geng et al., 2013).

1 $|\Delta a(x)| < J$

2 $\Delta b(x)^{-1} < K < 1$

3 $|w(t)| \leq W$

4 $b_0(x) = b(x) \neq 0$.

The control objectives are to track the reference signal in presence of external disturbances and bounded controller output, and formulation of total control input signal based on minimum-maximum values of nominal system parameters.

3 Design of control algorithms

3.1 Sliding mode control

To design the control input, the sliding function is selected as (Slotine and Li, 1991)

$$s(t) = \left(\frac{d}{dt} + \rho \right)^{n-1} + e(t) \tag{4}$$

where n is order of the system, the error signal is $e(t) = r(t) - c(t)$, $r(t)$ is the reference/ input excitation signal, $c(t)$ is the plant output signal and ρ is the positive gain-coefficient of sliding surface, i.e., $\rho > 0$. One would select ρ such that performance of the system is stable and error dynamics should confined onto the sliding manifold. The magnitude of control efforts depends on the value of ρ.

For second-order process plant with time derivative of equation (4),

$$\begin{aligned} \dot{s}(x) &= \rho\dot{e}(t) + \ddot{e}(t) \\ \varphi &= -\Delta a(x) - \{b_0(x) + \Delta b(x)\}u(t) + w(t) \end{aligned} \tag{5}$$

where $\varphi(x) = \rho e(t) + \dot{e}(t) - a_0(x)$.

The total control input is addition of discontinuous control and equivalent control as indicated by equation (6) (Eker, 2006)

$$u(t) = u_{eq}(t) + u_{dis}(t) \tag{6}$$

From estimated plant parameters and equations (4) and (5), the equivalent control is,

$$u_{eq}(t) = \frac{1}{b_0(x)}\varphi(x) \tag{7}$$

The switching control law is (Laware et al., 2018),

$$u_{dis}(t) = \frac{1}{b_0(x)}\omega \operatorname{sgn}\left(s(t)\right) \tag{8}$$

For the transition of error from reaching phase to sliding phase, control law must satisfy the stability conditions. Consider the direct Lyapunov function as (Slotine and Li, 1991; Eker, 2006; Laware et al., 2018; Khan and Spurgeon, 2006)

$$V(t) = \frac{1}{2}s^2(t) \tag{9}$$

with $\dot{V}(t) < 0$, $s(t)\dot{s}(t)$, $s(t) \neq 0$.

Therefore,

$$\begin{aligned} \dot{V}(t) &= s(t)\dot{s}(t) \\ &= s(t)\Delta a(x) - s(t)w(t) - s(t)\Delta b_0^{-1}(x)\varphi(x) - \omega\left|s(t)\right| - \Delta b(x)b_0^{-1}(x)w\left|s(t)\right| \\ &= -\left\{\omega(1-K) - J - W\right\}\left|s(t)\right| \\ &= -\left|s(t)\right|\left\{\omega(1-K) - J - W\right\} < 0 \end{aligned} \tag{10}$$

with the condition, $\omega > (J + W) / (1 - K)$, system is in reaching phase and sliding manifold converges to zero in afinite time. As Lyapunov function is negative semi-definite, the stability is guaranteed.

3.2 Global SMC

Consider global dynamic sliding surface in combination with function $h(t)$ as (Liu, 2006; Chang and Gao, 2010)

$$s_g(t) = \dot{e}(t) + \rho_g e(t) - h(t) \tag{11}$$

In which, $\rho_g > 0$, $h(t)$ is the function which converges to sliding manifold and satisfies the following conditions.

1 $h(0) = \dot{e}_0(t) + \rho_0 e_0(t)$

2 $h(t) \to 0$ as time approaches to infinity.

3 $h(t)$ is derivable

From above three conditions, $h(t)$ can be designed as

$$h(t) = h(0)e^{-kt} \tag{12}$$

Condition 1 represents an initial location of system states onto the sliding surface and e_0 is an initial magnitude of error. Condition 2 shows an asymptotic stability while condition 3 indicates the existence of sliding phase.

The first order process with dead-time is represented as (Parvat and Patre, 2017)

$$\frac{c(s)}{u(s)} = \frac{K}{(\tau s + 1)} e^{-ds} \tag{13}$$

In equation (13), K: static-gain of the process, τ: process time-constant, d: dead-time of the process, $c(s)$: transmitter output and $u(s)$: controller output.

The Taylor's series approximation for dead-time d yields,

$$\frac{c(s)}{u(s)} = \frac{K/\tau d}{s^2 + \left[\frac{\tau + d}{\tau d}\right] s + \frac{1}{\tau d}} \tag{14}$$

Estimated system parameters are: $A = \frac{\tau + d}{\tau t}$, $B = \frac{1}{\tau d}$ and $C = K / \tau d$.

Therefore, one has the relations as

$a_0(x) \equiv (A, B, C)$ and $b_0(x) \equiv C$ while $\Delta a(x) \equiv (\Delta A, \Delta B)$ and $\Delta b(x) \equiv \Delta C$.

In time-domain, equation (14) can be represented as

$$\ddot{c}(t) + \frac{\tau + d}{\tau d}\dot{c}(t) + \frac{1}{\tau d} c(t) = \frac{K}{\tau d} u(t) \tag{15}$$

From equation (15), one has,

$$\ddot{c}(t) = -\frac{\tau + d}{\tau d}\dot{c}(t) - \frac{1}{\tau d} c(t) + \frac{K}{\tau d} u(t) \tag{16}$$

The total control input $u_g(t)$ in terms of minimum-maximum values of estimated system parameters and external disturbance W is,

$$\begin{aligned} u_g = {} & C_u \left[\dot{h}(t) - \rho_g \dot{c}(t)\right] + A_u \dot{c}(t) + B_u c(t) \left\{-\Delta C \left|\dot{h}(t)\right| + \Delta C \left|\rho_g \dot{c}(t)\right| + \Delta A \left|\dot{c}(t)\right| \right. \\ & \left. + \Delta B \left|c(t)\right| + W\right\} \operatorname{sgn}\left(s_g(t)\right) \end{aligned} \tag{17}$$

where $C_u = \frac{C_{\max} + C_{\min}}{2}$, $A_u = \frac{A_{\max} + A_{\min}}{2}$, $B_u = \frac{B_{\max} + B_{\min}}{2}$, $\Delta C = \frac{(C_{\max} - C_{\min})}{2}$, $\Delta A = \frac{(A_{\max} - A_{\min})}{2}$ and $\Delta B = (B_{\max} - B_{\min}) / 2$.

3.3 Stability verification

Differentiating equation (11), yielding,

$$\begin{aligned}\dot{s}_g(t) &= \ddot{e}(t) + \rho_g \dot{e}(t) - \dot{h}(t)(\\ &= \ddot{r}(t) - \ddot{c}(t) + \rho_g \left[\dot{r}(t) - \dot{c}(t)\right] \\ &= \ddot{r}(t) + A\dot{c}(t) + Bc(t) + Cu(t) + \dot{h}(t) + \rho_g \dot{r}(t) + \left(\ddot{r}(t) - \rho_g \dot{c}(t)\right) + W \\ &= C\Big[C^{-1}\left(\rho_g \dot{c}(t) - \dot{h}(t)\right) - C^{-1}\left(\ddot{r}(t) + \rho_g \dot{r}(t)\right) + u(t) + W\Big]\end{aligned} \tag{18}$$

From equations (17) and (18), yielding,

$$\begin{aligned}C^{-1}\dot{s}_g(t) &= C^{-1}\left[\rho_g \dot{c}(t) - \dot{h}(t)\right] - C^{-1}\left[\ddot{r}(t) + \rho_g \dot{r}(t)\right] - C_u\left[\rho_g \dot{r}(t) - \dot{h}(t)\right] \\ &\quad + C_u\left[\ddot{r}(t) + \rho_g \dot{r}(t)\right] - \left\{\Delta B\left|\rho_g \dot{r}(t)\right| + \Delta B\left|\dot{h}(t)\right|\right. \\ &\quad \left. + \Delta B\left|\ddot{r}(t) + \rho_g \dot{r}(t)\right|\right\}\operatorname{sgn}\left(s_g(t)\right] + W\operatorname{sgn}\left(s_g(t)\right) \\ &= \left(C^{-1} - C_u\right)\left(\rho_g \dot{c}(t) - \dot{h}(t)\right) - \Delta C\left|\rho_g \dot{c}(t) - \dot{h}(t)\right|\operatorname{sgn}\left(s_g(t)\right) \\ &\quad - \left(C^{-1} - C_u\right)\left(\ddot{r}(t) + \rho_g \dot{r}(t)\right) - \Delta C\left(\left|\ddot{r}(t) + \rho_g \dot{r}(t)\right|\operatorname{sgn}\left(s_g(t)\right)\right. \\ &\quad \left. + W\operatorname{sgn}\left(s_g(t)\right)\right)\end{aligned} \tag{19}$$

One has an expression,

$$\begin{aligned}C^{-1}\dot{V}(t) &= C^{-1}s_g(t)\dot{s}_g(t) \\ &= \left(C^{-1} - C_u\right)\left(\rho_g \dot{c}(t) - \dot{h}(t)\right)s_g(t) - \Delta C\left|\rho_g \dot{c}(t) - \dot{h}(t)\right|\left|s_g(t)\right| \\ &\quad - \left(C^{-1} - C_u\right)\left(\ddot{r}(t) + \rho_g \dot{r}(t)\right)\left|s_g(t)\right| - \Delta B\left|\ddot{r}(t) + \rho_g \dot{r}(t)\right|\left|s_g(t)\right| \\ &\quad + W\operatorname{sgn}\left|s_g(t)\right|\end{aligned} \tag{20}$$

Therefore,

$$C^{-1}\dot{V}(t) < W\left|s_g(t)\right| < 0 \tag{21}$$

i.e., $\dot{V}(t) < 0$. This implies that Lyapunov candidate function is negative semi-definite. Hence, the proof of stability.

To reduce the chattering effect, tangential hyperbolic function is used as switching control input (Laware et al., 2015; Laware et al., 2021; Mei and Ding, 2021; Ghogare et al., in press). The tangential hyperbolic function is used to avoid zero mean signals. It facilitates the faster convergence rate of sliding surface and error signal to zero.

$$u_{dis}(t) = \omega_g \tanh\frac{s_g(t)}{\beta} \tag{22}$$

where ω_g is the gain and β is the boundary layer thickness.

4 System description

As the controlled variable (level) changes, process gain and process time-constant changes. When level in the tank rises, process time-constant increases and process gain decreases. Thus, level control system becomes nonlinear process and studied as an

illustrator example to validate global SMC strategy. Figure 1 shows process and instrument diagram (P&ID) of laboratory level tank process. Real-life experimental setup consists of a basin, 230 volts, 50 Hz motor to vary the inlet flowrate to tank, a level transmitter (LT) to give 4–20 mA DC signal corresponding to 0–100% level, an interfacing NI 6024E data acquisition (DAQ) card with BNC 2120 connector and a personal computer (PC). The output of LT is given to analogue input (AI) of BNC 2120 connector through current to voltage converter circuit. The controller output is applied to analogue output (AO) of BNC 2120 connector and conditioned to 4–20 mA DC current as an input to variable frequency drive.

The specifications of experimental setup are: height of process tank is 26.5 cm, cross sectional area of tank is 66.4 cm^2, sensor sensitivity is 0.604 mA/cm and actuator sensitivity is $0.17\frac{cm^3}{sec./V}$. The control algorithm is developed in MATLAB 2009a. When the pump is turned ON, level reaches to 40% for an applied voltage of 5 V from 0% level. Figure 2 illustrates the open-loop plot for 17% level change which is curve-fitted step response of first order model with dead-time. The dotted red line and blue colour line in Figure 2 indicates the model output and process output respectively. The identified transfer function of process is,

$$G_p(s) = \frac{0.0826}{\left(s^3 + 1.14\,s^2 + 4.93\,s + 0.09381\right)} e^{-3.7\,s} \tag{23}$$

With the reduced-order model of equation (23) and Pade approximation of dead-time element, one would obtain process transfer function as

$$G_p(s) = \frac{0.0046}{\left(s^2 + 0.28\,s + 0.007143\right)} \tag{24}$$

In which, $A = 0.28$, $B = 0.007143$ and $C = 0.0046$ are nominal plant parameters as stated earlier. The classical SMC and global SMC structure of control methods are depicted in Figure 3.

Figure 1 The experimental setup

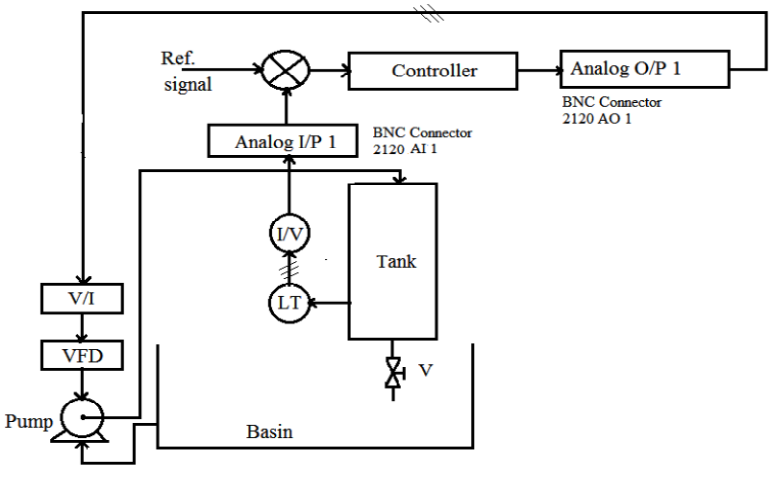

Figure 2 Open-loop step tests (see online version for colours)

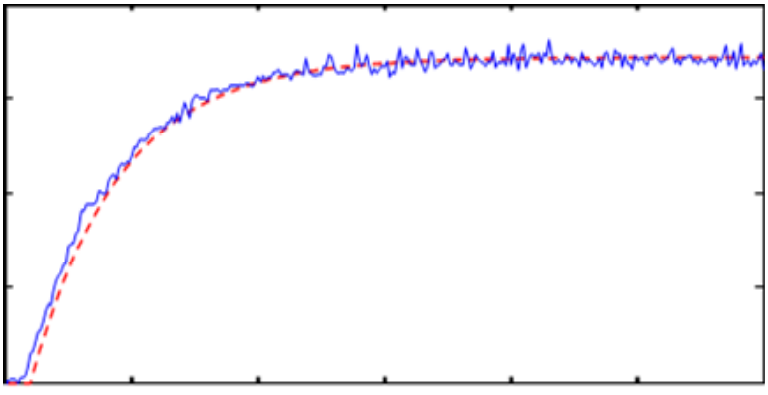

Figure 3 Structure of control methods

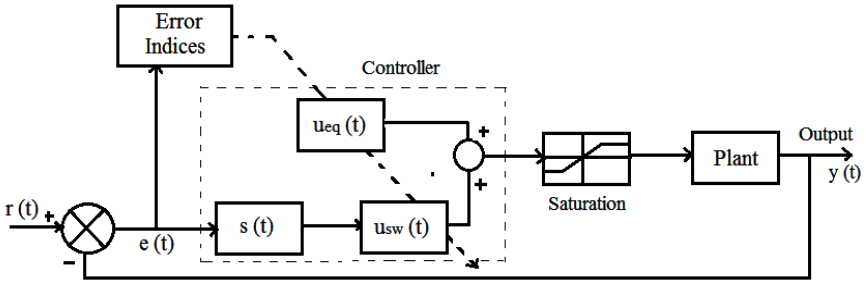

5 Real-time experimental results and discussion

The results of level control system are conferred for multilevel step changes and external disturbance. Figures 4(a) and 4(b) reveals the real-life experimental results of typical SMC. It shows that closed-loop response is profoundly oscillatory and never tracks exact set-point trajectory (±1.5% deviation). The control input exhibit severe chattering (variations from 1.293 volts to 4.074 volts) which causes unwanted wear and tear of actuator. The controller parameters for SMC are chosen to be: $\rho = 0.2$ and $\omega = 3$.

Figures 5(a) and 5(b) presents experimental results of GSMCr. For experimental validation, the preferential parameters selected are: $C_u = 0.0062$, $\Delta C = 0.00305$, $A_u = 0.375$, $\Delta A = 0.185$, $B_u = 0.0167$, $\Delta B = 0.0134$, $K = 50$, $W(t)_{\max} = 5$, initial error magnitude $e_0 = 7.6 \times 10^{-4}$, $s_0 = 0.0095$, $\rho_g = 0.6$, $\beta = 0.0008$, $C_{\max} = 0.0092$, $C_{\min} = 0.0031$, $A_{\max} = 0.56$, $A_{\min} = 0.19$, $B_{\max} = 0.03$ and $B_{\min} = 0.0032$ while lower and upper bounds on estimated parameters are: $A = [0.19\ 0.56]$, $B = [0.0032, 0.03]$ and $C = [0.0031, 0.0092]$.

From Figure 5(a), GSMCr response tracks the reference signal with ±0.5% deviation. The chattering signal variation is from 1.9 volts to 2.1 volts. Initially, it has maximum amplitude (5 V) for the period of 13.5 seconds.

Figure 4 SMC, (a) closed-loop response of level plant (b) variation of inlet flow rate as a controller output (see online version for colours)

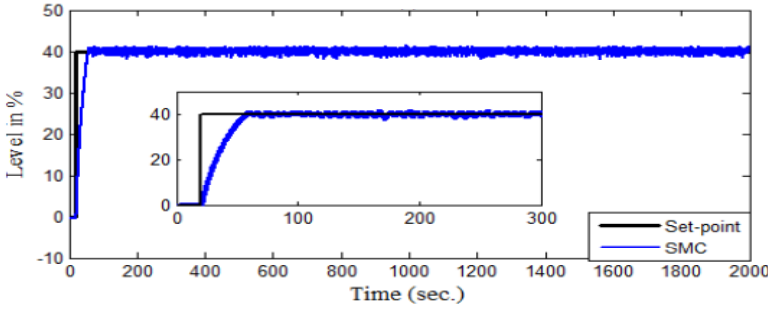

(a)

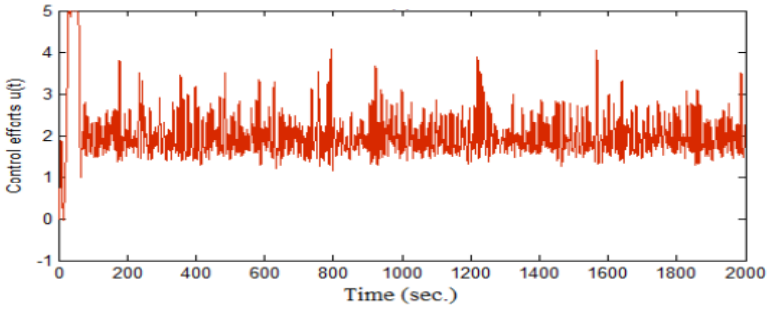

(b)

As depicted from Figures 4(b) and 5(b), chattering magnitude has been decreased considerably (SMC: ±2.8%, and GSMCr: ±0.3%). Thus, with the proposed strategy, chattering effect is alleviated. The learning curve of tracking error and sliding manifold for SMC are illustrated in Figures 6(a) and 6(b) respectively. The convergence of tracking error signal and sliding surface takes place in the neighbourhood of zero at 70 seconds and 65 seconds respectively. They do not converge exact to zero due to unmodelled dynamics of the system. Figures 7(a) and 7(b) shows convergence exactly to zero with smoother variations for GSMCrmethod. From Table 1, it can be seen that proposed strategy has better process speed, zero overshoot and reduced deviation in output variable (level). It has minimum convergence time for tracking error and sliding surface. It indicates alleviated chattering effect. Table 2 illustrates error-based performance indices for global SMC and typical SMC indicating better performance of proposed design.

Table 1 Performance comparison

Controller	*Settling time (sec.)*	*Rise time (sec.)*	*Overshoot %*	*Output deviation %*	*Variation of chattering signal (volts)*	*Error convergence to zero (sec.)*	*Sliding surface convergence to zero (sec.)*
GSMCr	54.16	29.6	0	±0.5	1.9 to 2.1	42.31	50.46
SMC	65	55	1.5	±1.5	1.293 to 4.074	70	65

Table 2 Performance indices: IAE: integral absolute error, ISE: integral square error, ISTAE: integral square time absolute error and ISECE: integral square error and control error

Controller	*IAE*	*ISE*	*ISTAE* 10^7	*ISECE* 10^4
GSMC	68.2	36.0	4.34	1.8
SMC	108.2	39.3	10.1	2.1

Figure 5 GSMCr, (a) closed-loop response of level plant (b) variation of inlet flow rate as a control signal (see online version for colours)

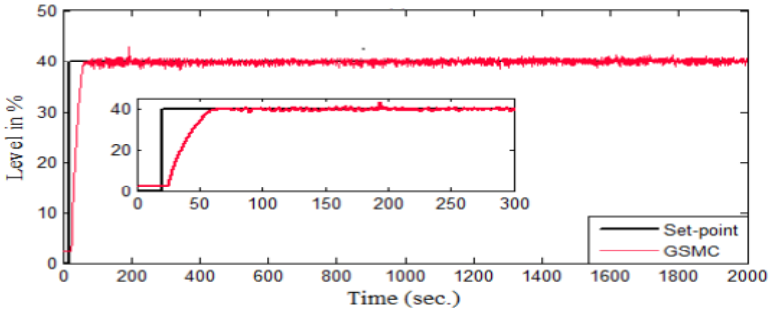

(a)

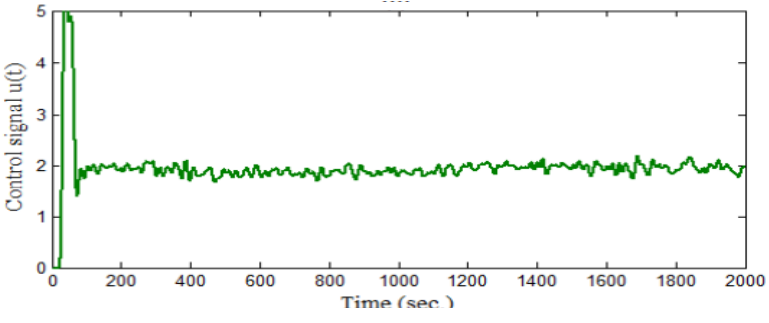

(b)

6 Robustness and disturbance rejection analysis

The control performance of a system with proposed algorithm has been analysed for system parameter variations, multi-level reference changes and external disturbances. The robustness to system parameter variations has been ensured for +25% change in process gain, +25% change in time-constant of process and –25% change in dead-time. Also, it is verified for set-point changes and realistic external disturbances. Figures 8(a), 8(b), 9(a) and 9(b) reveals the tracking performance of SMC and GSMCr with applied control input respectively. The set-point changes from 40% to 50% for the period of 600–1,000 seconds and from 40% to 34% for the period of 1,400–1,700 seconds. From Figures 8(a) and 8(b), one can observe that closed-loop response tracks the desired trajectory with large overshoot and undershoot (±2%). The control input exhibits a considerable amount of oscillations while Figures 9(a) and 9(b) explores extremely small oscillations about 0.5%. The magnitude of oscillation is less as compared to SMC.

Figure 6 SMC, (a) error signal (b) sliding surface (see online version for colours)

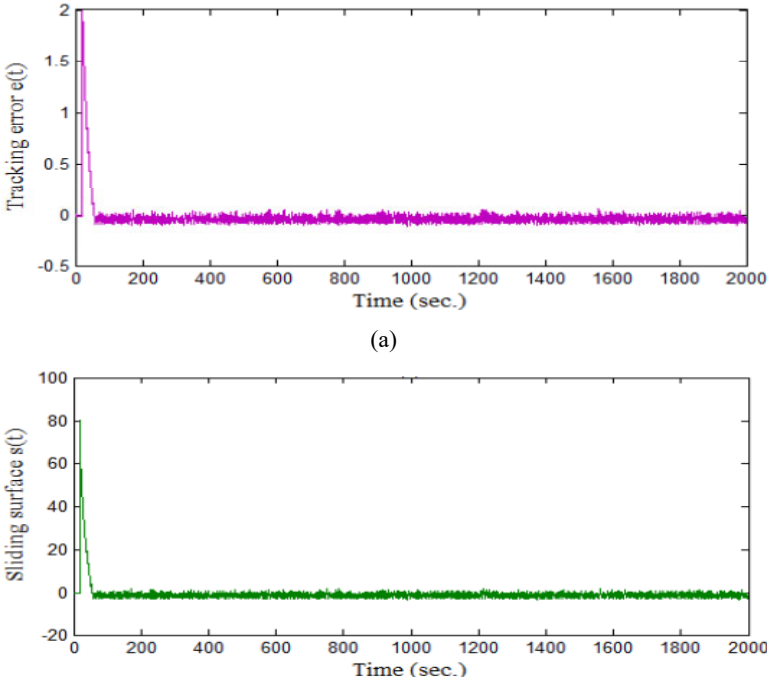

Figure 7 GSMCr, (a) error signal (b) sliding surface (see online version for colours)

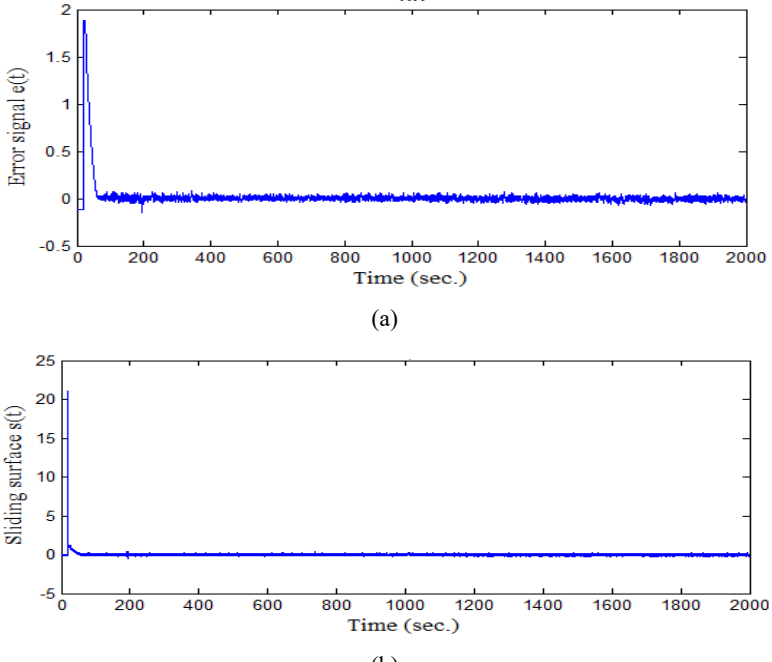

Figure 8 SMC, (a) multi-level change and disturbance rejection analysis (b) controller output (see online version for colours)

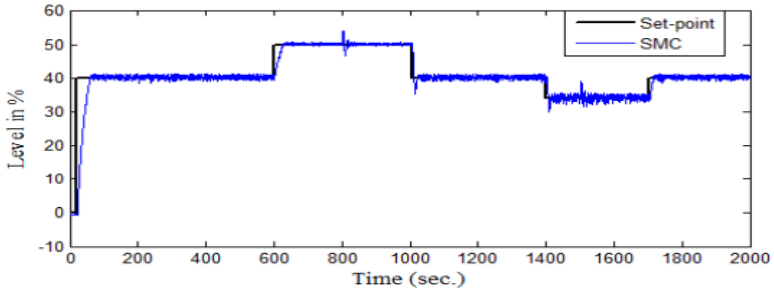

(a)

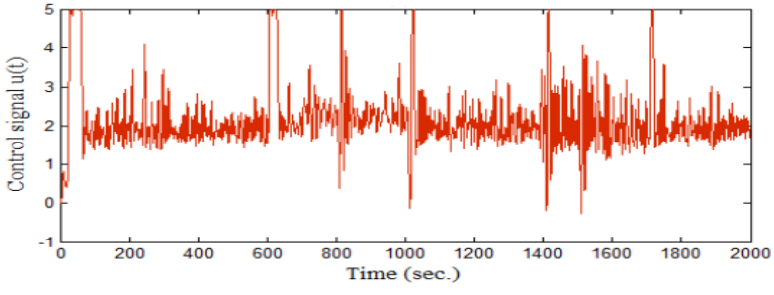

(b)

Figure 9 GSMCr, (a) multi-level change and disturbance rejection analysis (b) controller output (see online version for colours)

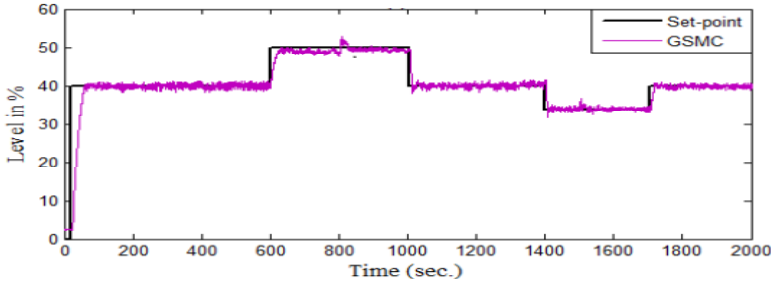

(a)

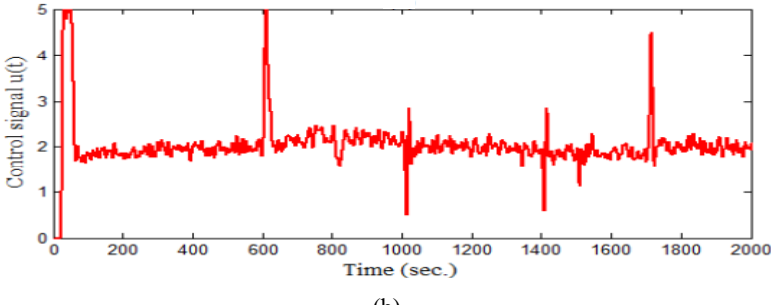

(b)

Figure 10 SMC, (a) error signal (b) sliding surface (see online version for colours)

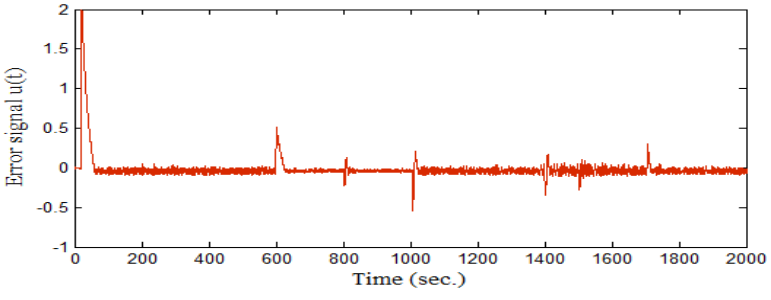

(a)

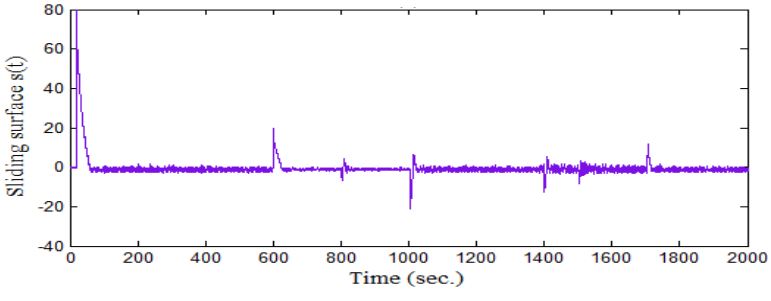

(b)

Figure 11 GSMCr, (a) error signal (b) sliding surface (see online version for colours)

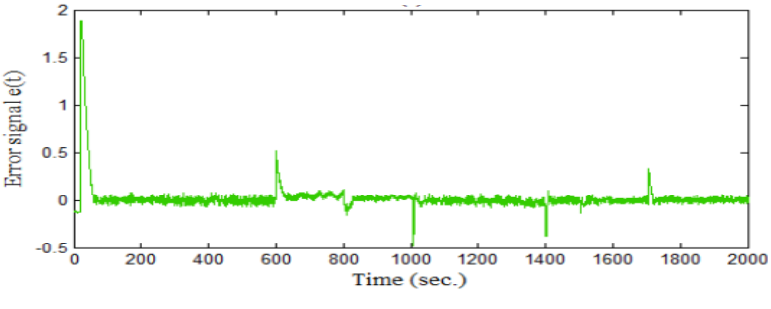

(a)

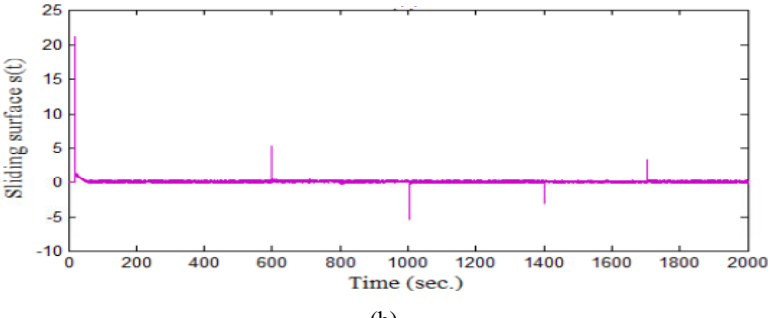

(b)

To test the robustness of controller to external disturbances, 5% water is added at 800 seconds and 1,500 seconds for the period of 20 seconds. This is equivalent to initiate the changes in dynamics of the system. The robustness is guaranteed by GSMCr. The corresponding error signal variations and trends of sliding surface are depicted in Figures 10(a), 10(b), 11(a) and 11(b) for classical SMC and global SMC algorithms respectively. For proposed control design method, smooth variations have been observed. The analysis reveals that proposed strategy tracks the desired reference signal comparatively at a faster rate than SMC. It has been observed that GSMCr reject the disturbances before 15 seconds in comparison with classical SMC.

7 Simulation example: second-order servo plant

Consider a servo plant as (Geng et al., 2013),

$$\ddot{x}(t) = a(x) + b(x)u(t) + w(t) \tag{25}$$

In which, $x(t)$ is position signal, $a(x) = -30\ \dot{x}$, $b(x) = 30$ and $w(t) = 50\sin(t)$.

The parameters for classical SMC selected are to be: $\rho = 15$ and $\omega = 1.5$. Figures 12(a), 12(b) and 12(c) devises the performance of closed-loop system. From Figure 12(a), the error between reference signal and position tracking signal is 1.8×10^{-4}. Figure 12 (b) presents the control signal in which initial control magnitude is 60. The magnitude of control signal chattering is ±7.634. The sliding surface variation is explored in Figure 12(c) which is ±0.06269. Initial magnitude of sliding surface is 0.092.

The proposed method has been designed for the plant represented by equation (25) with the parameters selection as: $\rho_g = 10$, $h(0) = s(0)e^{-130t}$, $k = 130$, $W(t)_{\max} = 0.1$, initial error magnitude $e_0 = \dfrac{pi}{6}$, $W = 0.1$, $s_0 = 0$, $\beta = 0.05$ and $w(t) = 0.2\sin(6.28t)$. The function $g(x)$ combines the system parameters C_u, ΔC, A_u, ΔA, B_u and ΔB. The lower bound on $g(x)$ is selected as 0.8 while upper bound is selected as 1.3.

Figures 13(a), 13(b) and 13(c) presents the control performance of global SMC. From Figure 13(a), one can observe that tracking signal follows exactly the command signal after 0.2442 seconds with zero error. Figure 13(b) shows that initial control magnitude in control efforts is 31.66. It chatters in between ±0.62 while Figure 13(c) shows smooth variations of sliding surface as compared to typical SMC.

8 Conclusions

In this work, GSMCr algorithm has been developed and implemented in a real-life environment for a nonlinear level tank system against ±25% uncertainties, reference signal changes and external disturbances. The stability conditions are derived using direct Lyapunov candidate function. The tracking error and sliding surface of proposed technique offers faster convergence to reach equilibrium state as compared to typical SMC.

The conventional SMC shows ±1.5% deviation in controlled variable while GSMCr shows ±0.5% deviation. The chattering amplitude variation is ±2.8% and ±0.3% for conventional SMC and global SMC respectively. The results show that GSMCr alleviate chattering and ensures smooth sliding surface.

Figure 12 Simulation results of SMC, (a) estimated system response (b) control signal (c) sliding surface (see online version for colours)

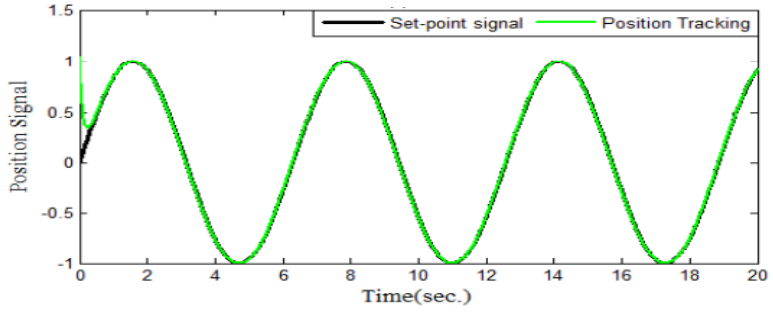

(a)

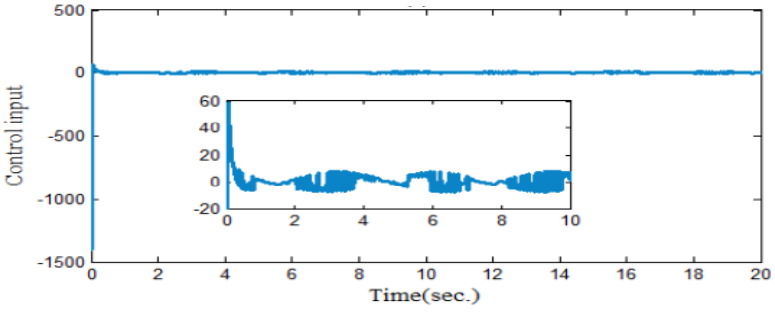

(b)

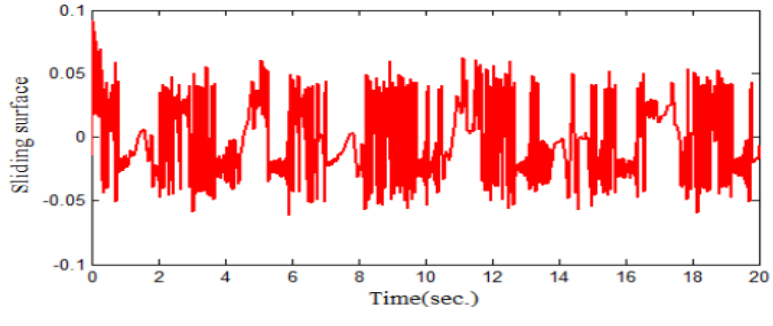

(c)

For SMC, more control energy is required for set-point tracking and disturbance response than GSMCr. classical SMC presents down peak at 1,000 seconds and 1,400 seconds whereas global SMC do not reveal such peak for step change response. It has been found that proposed method offers lesser rise time, settling time, deviation in controlled variable and zero overshoot compared to SMC. It is investigated that proposed strategy brings 33.33% improvement in a controlled performance of tank level control system and 10.71% chattering reduction in control signal while the simulation tests show 8.51% reduction in chattering with global SMC method as compared to classical SMC. The efficiency of proposed control design method is competent over SMC as seen from simulation tests conducted on second-order servo plant for sinusoidal input.

Figure 13 Simulation results of GSMCr, (a) estimated system response (b) control signal (c) sliding surface (see online version for colours)

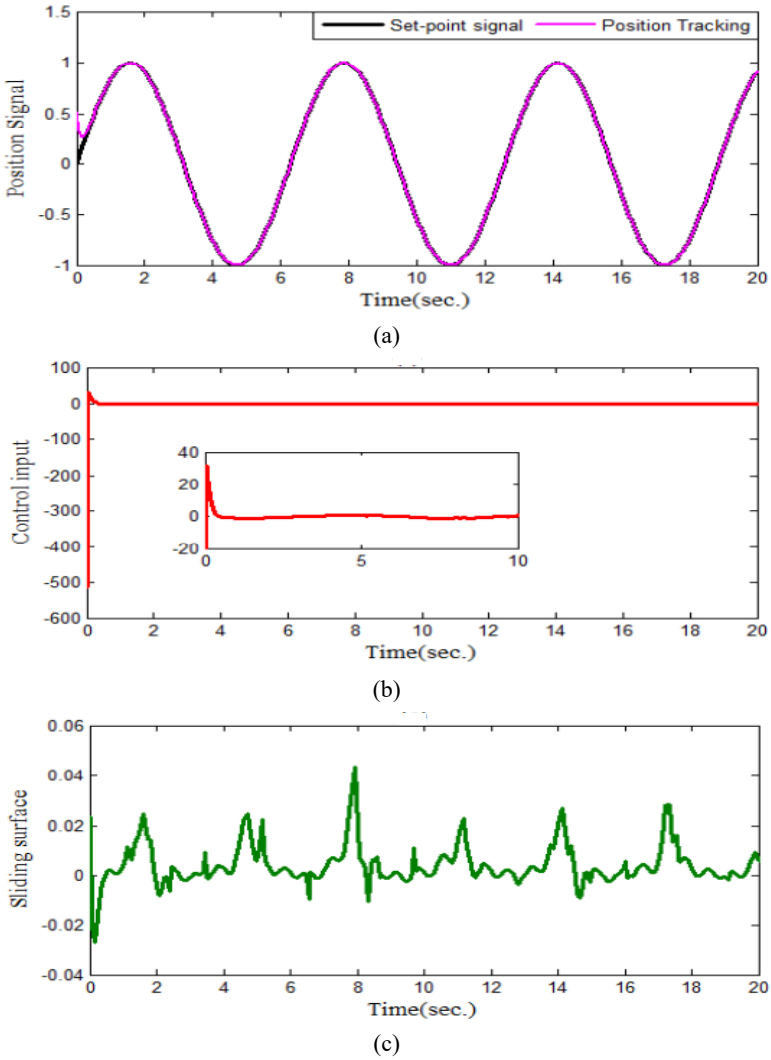

References

Anumula, T.N., Gouda, A., Jyothi, K., Kalpashree, N. and Veeranna, S.B. (2017) 'Wireless-based DC motor controlling and monitoring system', *International Journal of Systems, Control and Communications*, Vol. 8, No. 1, pp.72–88 [online] https://doi.org/10.1504/IJSCC.2017.081539.

Ashchepkov, L.T. (1983) 'Optimization of sliding motion in a discontinuous control', *Autom. Remote Cont.*, Vol. 44, No. 11, pp.30–37.

Cai, L., Chen, F.Y. and Lu, F.F. (2013) 'Global robust sliding mode tracking control for helicopter with input timedelay', *Advanced Materials Research*, pp.434–437 [online] https://doi.org/10.4028/www.scientific.net/AMR.846-847.434.

Chang, Y. and Gao, B. (2010) 'A global sliding mode controller design for an intra-aorta pump', *ASAIO Journal*, pp.510–516 [online] https://doi.org/10.1097/MAT.obo13e3181ede369.

Chern, T.L. and Wu, Y.C. (1992) 'An optimal variable structure control with integrated compensation for electrohydraullic position servo control system', *IEEE Trans. Ind. Electron.*, Vol. 39, No. 5, pp.460–464 [online] https://doi.org/10.1109/41.161478.

Choi, H-s., Park, Y-h., Cho, Y. and Lee, M. (2001) 'Global sliding-mode control: improved design for a brushless DC motor', *IEEE Control Systems Magazine*, Vol. 21, No. 3, pp.27–35 [online] https://doi.org/10.1109/37.924795.

Choi, S.B. and Park, D.W. (1994) 'Moving sliding surfaces for fast tracking control of second-order dynamical systems', *J. Dyn. Syst. Measure. Contr.*, Vol. 116, pp.154–158 [online] https://doi.org/10.1115/1.2900671.

Eker, I. (2006) 'Sliding mode control with PID sliding surface and experimental applications to an electromechanical plant', *ISA Transactions*, Vol. 45, No. 1, pp.109–118 [online] https://doi.org/10.1016/S0019-057(07)60070-6.

Emelyanov, S.V. (1967) *Variable Structure Control Systems*, USSER, Nauka, Moscow.

Errami, Y., Ouassaid, M. and Moaroufi, M. (2016) 'Design of variable structure control for wind energy system-based permanent magnet synchronous generator and operating under different grid conditions', *Internal Journal of Systems, Control and Communication*, Vol. 7, No. 2, pp.164–185 [online] https://doi.org/10.1109/ICoCS.2014.7060996.

Gandhi, P. and Bhole, K. (2013) 'Characterization of 'Bulk Lithography' process for fabrication of three dimensional microstructure', *J. Micro Nano-Manuf.*, December, Vol. 1, No. 4, p.41002 [online] http://doi.org/10.1115/1.4025461.

Gandhi, P., Deshmukh, S., Ramtekkar, R., Bhole, K. and Baraki, A. (2013) 'On-axis' linear focused spot scanning micro stereo lithography system: opto mechatronic design, analysis and development', *Journal of Advanced Manufacturing Systems*, Vol. 12, No. 1, pp.43–68 [online] http://doi.org/10.1142/S0219686713500030.

Geng, J., Sheng, Y., Liu, X. and Liu, B. (2013) 'Second order time-varying sliding mode control for uncertain system', *2013 25th Chinese Control and Decision Control Conference (CCDC)*, pp.3880–3885 [online] https://doi.org/10.1109/CCDC.2013.6561626.

Ghogare, M.G., Kumar, S., Patil, L., Kumar, C. and Patil, Y. (in press) 'Experimental validation of optimized fast terminal sliding mode control for level control system', *ISA Transactions* [online] https://doi.org/10.1016/j.isatra/2021.08.007.

Gholipour, S., Kazemitabar, J., Alizadeh, M. and Minagar, S. (2021) 'Fractional dynamic sliding mode control for non-identical uncertain fractional chaotic systems', *International Journal of Systems, Control and Communications*, Vol. 12, No. 2, pp.132–147 [online] https://doi.org/10.1504/IJSCC.2021.114600.

Hung, J.Y., Gao, W. and Hung, J.C. (1993) 'Variable structure control: a survey', *IEEE Trans. Ind. Electron.*, Vol. 40, No. 1, pp.2–25 [online] https://doi.org/10.1109/41.184817.

Itkis, U. (1976) *Control Systems of Variable Structure*, Wiley, New York.

Khan, M.K. and Spurgeon, S.K. (2006) 'Robust MIMO water level control using second-order sliding mode control', *Control. Eng. Pract.*, Vol. 14, No. 1, pp.375–386 [online] https://doi.org/10.1016/J.CONENGPRAC.2005.02.001.

Laware, A.R., Navthar, R.R., Bandal, V.S. and Talange, D.B. (2021) 'Global optimization of second-order sliding mode controller parameters using a new sliding surface: an experimental verification to process control system', *ISA Transactions* [online] https://doi.org/10.1016/j.isatra/2021.08.013.

Laware, A.R., Talange, D.B. and Bandal, V.S. (2018) 'Evolutionary optimization of sliding mode controller for level control system', *ISA Transactions*, Vol. 83, pp.199–213 [online] https://doi.org/10.1016/j.isatra/2018.08.011.

Liu, J. (2006) 'Nominal model-based sliding mode control with backstepping for 3-axis flight table', *Chinese Journal of Aeronautic*, Vol. 19, No. 1, pp.42–46 [online] https://doi.org/10.1016/s1000-9361(11)602690.

Lu, Y.S. and Chen, J.S. (1995) 'Design of global sliding-mode controller for a motor drive with bounded control', *Int. J. Contr.*, Vol. 62, No. 5, pp.1001–1019 [online] https://doi.org/10.1080/00207179508921579.

Lu, Y.S. and Chen, J-s. (2007) 'Design of global sliding mode controller for a motor drive with bounded control', *Int. J. of Control*, Vol. 62, No. 5, pp.1001–1019.

Lu, Y-S. and Chiu, C-W. (2009) 'Global sliding mode control with generalized sliding dynamics', *Asian Journal of Control*, Vol. 11, No. 4, pp.449–456.

Mei, K. and Ding, S. (2021) 'Second-order sliding mode controller design subjected to an upper-triangular structure', *IEEE Transactions on System, Man, and Cybernetics Systems*, Vol. 51, No. 1, pp.497–507 [online] https://doi.org/10.1109/TSMC.2018.2875267.

Mobayen, S. (2015) 'A novel global sliding mode control based on exponential reaching law for a class of underactuated system with external disturbances', *J. Comput., Nonlinear Dynam*., Vol. 11, No. 2, p.21011 [online] https://doi.org/10.1115/1.4031087.

Parvat, B.J. and Patre, B.M. (2017) 'Fast terminal sliding mode controller for square multivariable processes with experimental application', *Int. J. Dynam. Control*, Vol. 5, pp.1139–1146 [online] https://doi.org/10.1007/s40435-016-0262-x.

Singh, K. and Padhy, P.K. (2017) 'Second order sliding mode PI-PD controller for inverted pendulum', *International Journal of Systems, Control and Communications*, Vol. 8, No. 3, pp.217–229 [online] https://doi.org/10.1504/IJSCC.2017.085495.

Slotine, J.J. and Li, W. (1991) *Applied Non-Linear Control*, Prentice Hall Inc., Englewood Cliffs, New Jersey.

Slotine, J.J.E. and Spong, M.W. (1985) 'Robust robot control with bounded input torques', *J. Robot Syst.*, Vol. 2, No. 4, pp.329–351 [online] https://doi.org/10.1002/rob.4620020402.

Uswarman, R., Cahyadi, A.I. and Wahyunggoro, O. (2014) 'Design and implementation of magnetic levitation system controller using global sliding mode control', *Mechatronics, Electrical Power and Vehicular Technology*, Vol. 5, pp.17–26 [online] https://doi.org/10.14203/j.mev.2014.v5.17-26.

Xiu, C., Hou, J., Xu, G. and Zag, Y. (2017) 'Improved fast global sliding mode control based on the exponential reaching law', *Advances in Mechanical Engineering*, Vol. 9, No. 2, pp.1–8 [online] https://doi.org/10.1177/1687814016687967.